Image Cover Sheet

CLASSIFICATION	SYSTEM NUMBER
UNCLASSIFIED	507273

TITLE

ADAPTIVE BEAMFORMING AGAINST REVERBERATION FOR A THREE-SENSOR ARRAY

System Number:

Patron Number:

Requester:

Notes:

DSIS Use only:

Deliver to: FF

Adaptive beamforming against reverberation for a three-sensor array

Joseph N. Maksym and Michael Sandys-Wunsch
Defence Research Establishment Atlantic, 9 Grove St., Dartmouth, Nova Scotia B2Y 3Z7, Canada

(Received 16 September 1996; revised 11 August 1997; accepted 22 August 1997)

Two algorithms for beamforming and bearing estimation of echoes from an active sonar transmission in a strongly reverberant bistatic environment are described. The receiving array consists of a single omnidirectional sensor and two collocated orthogonal dipole sensors, and is deployed in a bistatic configuration. Both beamforming algorithms are based on minimum-variance techniques. The first algorithm matches the pattern of the minimum-variance beamformed data with that expected from an impulse at a known bearing. The second algorithm reforms the sensor data from the minimum-variance beam response. Fixed-coefficient limaçon beamforming is then applied to estimate the beam power map with reduced reverberation. The detection performance of both techniques is evaluated by injection of a synthetic target echo into experimental reverberation data. The results suggest an enhanced array gain against reverberation of the order of 3 dB for reasonable values of signal strength and probability of false alarm, compared to a direct application of fixed-coefficient limaçon beamforming. The root-mean-squared bearing error for both techniques is reduced significantly, when compared to the limaçon beamformer, by factors varying from 2 to 5. [S0001-4966(97)03612-6]

PACS numbers: 43.30.Vh, 43.30.Bp, 43.30.Cq [SAC-B]

INTRODUCTION

The problem of particular interest in this paper is the detection and bearing estimation of target echoes in strongly anisotropic reverberation fields characteristic of bistatic active sonars operating in shallow water.[1–3] Although bistatic reverberation models capable of predicting the average background in bistatic active sonar are now highly developed,[4] such models depend on knowledge of environmental parameters, and may not always provide the accuracy required for optimum beamforming and the setting of detection thresholds. As a consequence, there is much interest in data-adaptive methods that can estimate the reverberation background from the sensor signals themselves.

This work is an examination of two adaptive beamforming techniques in a reverberation-limited active sonar environment for a receiver consisting of an omnidirectional sensor and two collocated orthogonal dipole sensors. Both techniques are based on the minimum variance distortionless response (MVDR) beamformer.[5] The first is the pattern correlator (PATCOR) processor, which is a three-step process involving adaptive beamforming, response identification, and correlation. The second is the directional interference limited beamspace energy reformation technique (DILBERT) transform, a process for calculating a transformation matrix that reforms the sensor time series into equivalent time series with reduced directional interference. Of interest is the receiver performance for the detection of an echo in a given direction, as well as the root-mean-squared (rms) error of the estimate of the associated bearing.

The current literature in adaptive beamforming includes application of MVDR to topics as diverse as sonar performance prediction,[6] consideration of the detection process in a structured noise background,[7] and the general treatment of rank reduction and signal enhancement.[8,9] Here, we wish to apply some of these concepts to the bistatic reverberation scenario illustrated schematically in Fig. 1 for a three-sensor receiving array consisting of an omnidirectional sensor and two orthogonal dipoles. With this configuration, apart from a possible signal arrival directly along the transmitter–receiver axis, reverberation at any particular instant during a ping arises from reflecting points on an ellipsoid that has the transmitter and receiver as the two foci. This fact, along with the strength and distribution of reflections from points on the ellipsoid, determines the directional character of bistatic sonar reverberation. Directionality of the reverberation field is important for the performance of the adaptive beamformers introduced in this paper. Bathymetric features complicate this reverberation distribution, but will not be considered in this work. It is convenient for analysis to estimate the direction of the transmitter–receiver axis, and to measure bearings relative to this reference axis as shown schematically in Fig. 2. One can then examine detection performance using data measured at receivers placed in a number of different locations by injecting signals at a known bearing relative to this reference axis.

To evaluate the two beamformers an experimental reverberation data set was recorded with receivers located over a wide area. A large number of transmissions, involving several waveforms over a wide band, were measured on each receiver. The transmitter–receiver geometries were diverse, ensuring that a variety of reverberation fields were included. Synthetic signals were then added at known values of bearing and signal-to-noise ratio (SNR). Receiver-operating characteristic (ROC) and rms bearing-estimation errors were directly measured with this data set. The fixed-coefficient limaçon beamformer described below was used as a benchmark both for the detection and for the bearing estimation problem.

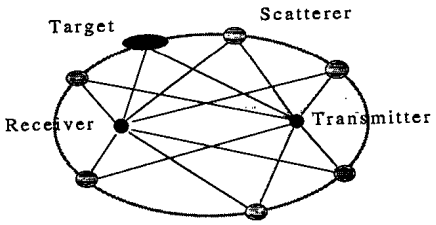

FIG. 1. Bistatic reverberation scenario.

For the long range bistatic sonar geometry that was used to gather the data (projector at least ten water depths from the sensor) it is reasonable to assume that almost all the reverberation arrives near the horizontal plane. This assumption allows us to simplify the subsequent development of the adaptive algorithms in this paper within a two-dimensional framework.

This paper is organized as follows. The fixed-coefficient limaçon beamformer and the two adaptive beamformers are outlined in Sec. I. The test data set and the results are described in Sec. II. Conclusions on the usefulness and limitations of these techniques are drawn in Sec. III.

I. THEORY

The starting point for the discussion of the beamformers is the output of a matched filter, with the signal of interest showing up as a sharp peak against a slowly varying background of reverberation. In the implementation used in this work the sensor data are first bandpass filtered with a finite impulse response (FIR) filter, and then matched filtered with a replica of the waveform.

Data-adaptive beamforming of matched filter output, rather than the raw sensor time series, brings with it the important advantage that the contribution of ambient noise not correlated with the transmitted waveform is reduced by the bandwidth-time (BT) product of the waveform. If raw sensor data were used instead, isotropic ambient noise would likely dominate, resulting in MVDR beams similar to limaçons.

A. The limaçon beamformer

The standard fixed-coefficient beamformer for the sensor configuration in this paper is the limaçon. Its power response is given by

$$p_\xi = \langle ([(1-\alpha),\ \alpha \sin \xi,\ \alpha \cos \xi]\mathbf{x})^2 \rangle_s, \tag{1}$$

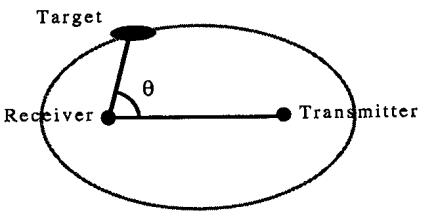

FIG. 2. Sensor geometry for the receiver. The angle of the direct arrival is used as a reference to realign the orthogonal dipole sensors.

where $\langle\ \rangle_s$ denotes a time average over the expected duration of the signal, ξ is the steering direction, and α is a parameter governing the shape of the response. With $\alpha = 0.5$ the result is a cardioid response pattern. We have found, for the experimental data in this paper, that $\alpha = 0.75$ is a good compromise, and this value will be used for the limaçon beamformer in this work. The resulting beam pattern has a broad main lobe somewhat narrower than that of the cardioid, and a backlobe that is 6 dB down from the main lobe.

A rough target bearing estimate $\hat{\phi}$ is taken from the peak of the beam response,

$$\hat{\phi} = \max_{\xi} \{p_\xi\}. \tag{2}$$

In order to improve precision, at the expense of an increase in variance, a parabolic interpolator is applied. Suppose the power detected in beam ϕ is p_1, and the power in the beams to either side is p_0 and p_2. Then, in terms of these powers and the angular spacing $\Delta\phi$ between beams the interpolated bearing estimate $\hat{\phi}_i$ is given by

$$\hat{\phi}_i = \hat{\phi} + \frac{1}{2} \Delta\phi \frac{p_2 - p_0}{2p_1 - p_0 - p_2}. \tag{3}$$

A total of 24 beams were formed so as to be consistent with the number of beams used in the two adaptive beamformers, although this is considerably more than is necessary because the main lobe of the limaçon beamformer is quite broad.

B. The PATCOR processor

The PATCOR processor is based on MVDR beamforming[5] in a number of equispaced steering angles ξ. Denote the response of the omnidirectional and the orthogonal dipole sensors to a plane wave incident at angle ξ by $\mathbf{s}_\xi$:

$$\mathbf{s}_\xi = [1, \sin \xi, \cos \xi]^T. \tag{4}$$

The MVDR beamforming vector $\mathbf{w}_\xi^0$ steered to angle ξ is then obtained in terms of the correlation matrix $\mathbf{Q}$ and the vector $\mathbf{s}_\xi$,

$$\mathbf{w}_\xi^0 = \frac{\mathbf{Q}^{-1}\mathbf{s}_\xi}{\mathbf{s}_\xi^T \mathbf{Q}^{-1} \mathbf{s}_\xi}, \tag{5}$$

where $\mathbf{Q} = \langle \mathbf{x}\mathbf{x}^T \rangle_t$ is the data correlation matrix. The angular brackets $\langle\ \rangle_t$ denote a time average. Note that the reverberation background changes considerably over time, and it is necessary to consider this nonstationarity when selecting an interval over which to estimate the correlation matrix. The time interval for averaging this matrix should be short compared to that over which the reverberation directionality changes, which is of the order of the transmitter–receiver propagation time. It should, however, be long compared to the expected echo width, which for matched filter data is of the order of the reciprocal bandwidth. In this work the time constant for obtaining the $\mathbf{Q}$ matrix is taken as 1500 independent samples. The MVDR coefficients are constant for a given window of data, but change as the next window is processed. For continuity, these data windows were overlapped by 50% in this work. In order to reduce the effect of strong reverberation peaks, we normalize the MVDR re-

sponse across bearing by dividing $\mathbf{w}_\xi^0$ by the average long term root power,

$$\mathbf{w}_\xi = \frac{\mathbf{w}_\xi^0}{\sqrt{\mathbf{w}_\xi^{0T}\mathbf{Q}\mathbf{w}_\xi^0}}. \tag{6}$$

Normalization of the average background across bearing is similar to the spectral prewhitening commonly used in the design of matched filters for signals in colored noise. Its use here is, to the authors' knowledge, novel. Besides ensuring a more isotropic background for the detection and bearing estimation of target echoes, it normalizes the reverberation background with time during the ping.

Having obtained a set of beamformers $\{\mathbf{w}_\xi\}$ indexed by equispaced bearings ξ, the next step is to calculate the power response for signal-direction vectors in the set $\{\mathbf{s}_\theta\}$ indexed by equispaced bearings θ. The response of the beamformer steered at direction ξ to a signal incident at θ is given by $|\mathbf{w}_\xi^T\mathbf{s}_\theta|^2$. We found by experiment that 24 values of ξ and an equal number for θ was sufficient for stable response of the PATCOR processor.

In the final step sensor data are processed with the above beamformers in a time window matched to the signal duration, yielding the set of average power responses $\{\langle|\mathbf{w}_\xi^T\mathbf{x}|^2\rangle_s\}$. This set, considered as a vector indexed by ξ, is compared by statistical correlation with each of the response vectors for signal directions in the set $\{\mathbf{s}_\theta\}$. A positive correlation for a particular $\mathbf{s}_\theta$ is indicative of the presence of signal power in direction θ. Since statistical correlation produces values in the range $[-1,1]$, the correlator output was first shifted to the range $[0,2]$ and scaled by one-half the signal power $\mathbf{w}_\theta^T\mathbf{Q}_s\mathbf{w}_\theta$. The full expression for the PATCOR output p_θ is given by

$$p_\theta = \frac{1}{2}\mathbf{w}_\theta^T\mathbf{Q}_s\mathbf{w}_\theta\left[1+\frac{\Sigma_\xi(\langle|\mathbf{w}_\xi^T\mathbf{x}|^2\rangle_s-\langle\langle|\mathbf{w}_\xi^T\mathbf{x}|^2\rangle_s\rangle_\phi)(|\mathbf{w}_\xi^T\mathbf{s}_\theta|^2-\langle|\mathbf{w}_\xi^T\mathbf{s}_\theta|^2\rangle_\phi)}{\sqrt{\Sigma_\xi[\langle|\mathbf{w}_\xi^T\mathbf{x}|^2\rangle_s-\langle\langle|\mathbf{w}_\xi^T\mathbf{x}|^2\rangle_s\rangle_\phi]^2\Sigma_\xi[|\mathbf{w}_\xi^T\mathbf{s}_\theta|^2-\langle|\mathbf{w}_\xi^T\mathbf{s}_\theta|^2\rangle_\phi]^2}}\right], \tag{7}$$

where $\langle\ \rangle_\phi$ denotes an average over all bearing terms. The bearing estimate is taken from the peak of p_θ as in Eq. (2), and parabolic interpolation is applied as in Eq. (3).

C. The DILBERT transform

The DILBERT transform is defined here. Essentially, it is a technique for "whitening" the average background interference across bearing, and is followed in this work by a limaçon beamformer. The MVDR coefficients defined by Eq. (6) provide a reverberation-normalized, minimum-variance estimate of the energy as a function of direction. We can recombine these bearing energies to produce sensor data with the dominant reverberation power reduced. Because the signal is of much smaller duration than the reverberation, it does not contribute significantly to the $\mathbf{Q}$ matrix, and hence is not rejected by the resulting MVDR beamformer. In order to obtain a good bearing estimate, we impose the constraint of minimizing the rms deviation from a delta-function response to a unit amplitude signal incident from direction θ. Such a sharp response is not possible with our receiver which has only three degrees of spatial freedom, but can be approximated in a least squares sense. This translates into minimizing the functional

$$F = \sum_\theta |\mathbf{v}_\xi\mathbf{w}_\xi^T\mathbf{s}_\theta - \delta(\xi-\theta)\sqrt{\mathbf{w}_\xi^T\mathbf{Q}\mathbf{w}_\xi}\mathbf{s}_\xi|^2, \tag{8}$$

where $\mathbf{v}_\xi$ is the weighting vector for reforming the sensor data from energy in direction ξ, and $\delta(\xi-\theta)$ is a Dirac delta function.

Minimizing F with respect to the beam weighting vector $\mathbf{v}_\xi$ yields the equation

$$\mathbf{v}_\xi = \frac{\mathbf{s}_\xi}{\mathbf{w}_\xi^T\mathbf{Q}_i\mathbf{w}_\xi}, \tag{9}$$

where $\mathbf{Q}_i$ is the normalized correlation matrix for two-dimensional isotropic noise:

$$\mathbf{Q}_i = \begin{bmatrix} 1 & 0 & 0 \\ 0 & 0.5 & 0 \\ 0 & 0 & 0.5 \end{bmatrix}. \tag{10}$$

Application of a set of MVDR beamformers indexed by ξ to the sensor data, followed by recombination of these beams by the weighting vectors $\mathbf{v}_\xi$, is equivalent to multiplication of the sensor data by the matrix $\mathbf{H}$,

$$\mathbf{H} = \sum_\xi \frac{\mathbf{s}_\xi\mathbf{w}_\xi^T}{\mathbf{w}_\xi^T\mathbf{Q}_i\mathbf{w}_\xi}. \tag{11}$$

In this work 1000 bearing terms are used to form the sum in Eq. (11) in order to ensure a stable estimate of $\mathbf{H}$. The recombined sensor data can be subsequently beamformed with a limaçon beamformer as in Eq. (1), and the signal bearing estimated from the peak as before.

II. TEST DATA SET AND RESULTS

For the evaluation of detection performance and bearing estimation error, a data set consisting of reverberation from a series of FM sweeps was collected on a number of three-sensor receivers. A large number of receivers in a variety of tactical geometries with respect to the transmitter, and several different transmitted waveforms were used to obtain a diverse data set.

Bandpass filtering and matched filtering were applied to the time series from each sensor. A smoothed estimate of the

power in the omni sensor was made in order to provide a basis for computing the SNR for purposes of synthetic signal injection. The bearing of the direct arrival of energy from the transmitter was measured by means of the limaçon beamformer, and used as a reference axis from which all bearings were measured in order to observe the effect of beamformer performance as a function of the angle off the main reverberation axis.

The time resolution of the matched filter output is approximately the reciprocal bandwidth. When considering the number of independent samples used in various stages of the processing, we have taken this resolution into account, assuming f_N/B samples are correlated, where f_N is the Nyquist frequency, and B the bandwidth. Data within a fixed window of 7500 independent samples were extracted from each transmission. For the purpose of the PATCOR processor and the DILBERT transform, 50% overlapped windows of 1500 samples duration were used to estimate the **Q** matrices. For all three beamformers averaging of the outputs for signal detection was performed over 30 sample intervals.

In preparing the recorded reverberation data for the evaluation of performance the reverberation noise power in the omnidirectional sensor was first measured. Then, data examples were created at desired SNR by adding a constant power level signal to the reverberation data. As a consequence, the signal-plus-noise statistics of the test data set were those of fluctuating background plus a constant strength signal. The ROC curves were obtained by incrementing a counter if the signal-plus-noise power at a processor output exceeded an adjustable detection threshold (DT). The number of threshold crossings were then divided by the total number of trials to form an estimate of P_D. The probability of false alarm P_{FA} was estimated by recording the number of crossings of the noise level over the same DT. The rms bearing errors were obtained from the average squared difference between the measured bearing of the inserted signal and the true bearing.

A. ROC curves

The ROC curves for all three beamformers are shown in Fig. 3. The false alarm probability P_{FA} is plotted in logarithmic scale along the x axis, and the detection probability P_D in increasing logarithmic scale along the y axis. The range of SNRs for the injected signal is from -6 dB to $+3$ dB with respect to reverberation power measured in the omni channel. Note that a smoothed estimate of power in the omni channel is used for this purpose, in order to avoid effects due to the large fluctuations characteristic of reverberation. The bearings of the synthetic signal vary from 0 to 360 degrees in 60-degree increments. Because the results are symmetric about the transmitter–receiver axis, only the curves for signals at 0, 60, 120, and 180 degrees are shown.

It should be pointed out that the reverberation background was nonstationary, so that these results represent an average over a time window, and it is likely that the distribution of reverberation fluctuations changed somewhat over this window. It should also be pointed out that the data set did not include anomalous reverberation returns, for example from large bathymetric features. The signal-plus-noise detection statistics were deduced for a signal injected in a single direction. This is a cued detection problem, appropriate when the beamformer performance in a given direction is to be optimized.

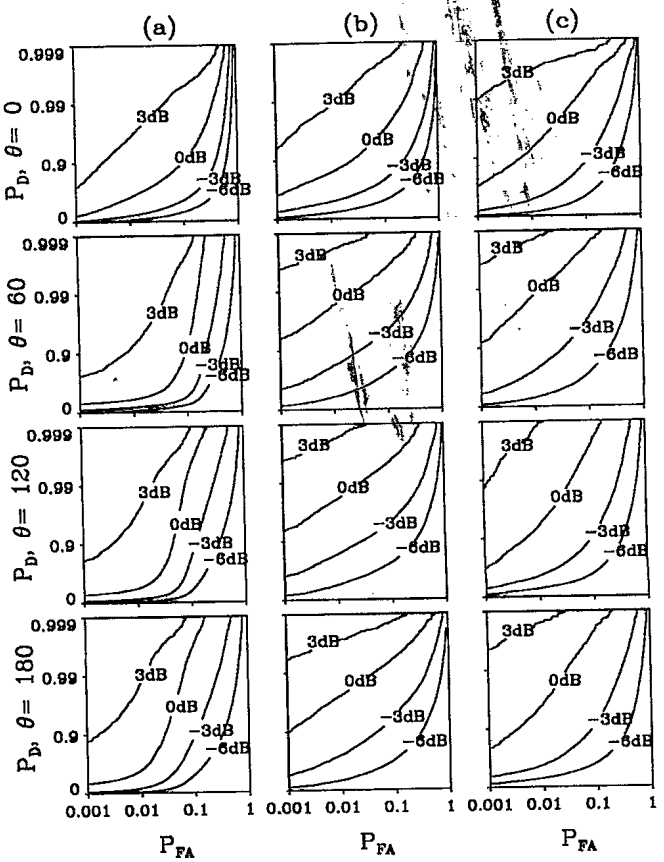

FIG. 3. ROC curves for the three beamformers; (a) limaçon; (b) PATCOR; and (c) DILBERT transform plus limaçon. The signal angle θ is taken at 0, 60, 120, and 180 degrees with respect to the transmitter–receiver axis. The SNR is with respect to the power measured in the omni sensor.

The ROC curves for the PATCOR processor show a considerable improvement over a processor employing a limaçon beamformer. They indicate an average performance gain of approximately 3 dB at a P_{FA} of 0.01, with the caveat that at the lower SNRs the differences in performance is reduced. The ROC curves for the DILBERT transform followed by limaçon beamforming show similar improvements over those of the limaçon beamformer alone. Again, at very low SNRs the difference in performance is reduced.

Detection performance is illustrated as a function of SNR for $P_{\mathrm{FA}}=0.01$ in Fig. 4. Separate plots are made for signal bearings θ at 0, 60, 120, and 180 degrees. The two adaptive beamformers show the same P_D as the limaçon at SNRs that are lower by 3–6 dB.

B. rms bearing errors

We compare the bearing-estimation performance of the three beamforming systems in Fig. 5. The estimator based on the limaçon beamformer tends to lock onto the background reverberation, producing a bearing estimate independent of the signal, but with very low variance. The two adaptive beamformers exhibit low bias, but considerably higher vari-

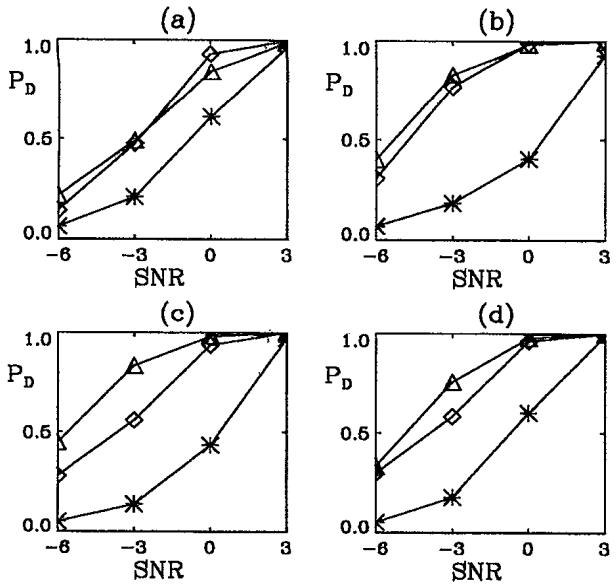

FIG. 4. P_D as a function of SNR, for a P_{FA} of 0.01. The symbols are as follows: *—limaçon beamformer; ◇—PATCOR processor; △—DILBERT transform plus limaçon. The four panels correspond to signal bearings θ at: (a) 0; (b) 60; (c) 120; and (d) 180 degrees.

ance, especially for low SNR signals. The rms bearing error takes both types of error into account and thus summarizes overall performance. A separate curve is plotted for each of four different values of signal bearing relative to the reference axis.

Using the limaçon-based estimator as a benchmark, Fig. 5 indicates variable and often large reductions in rms bearing error achieved by the adaptive systems. For signal bearings on the projector–receiver axis the adaptive systems show no improvement, while for the other signal directions reductions up to 4× for the PATCOR processor, and up to 3× for the

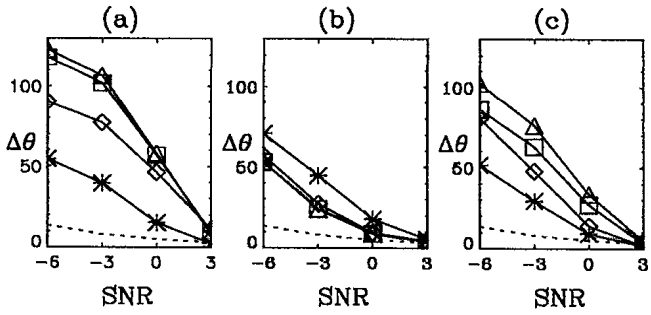

FIG. 5. rms bearing errors for the three beamformers; (a) limaçon beamformer; (b) PATCOR processor; and (c) DILBERT transform plus limaçon beamformer. The symbols are as follows: *—$\theta=0$; ◇—$\theta=60$; △—$\theta=120$; □—$\theta=180$; ⋯—CRLB.

DILBERT processor are achieved for SNRs below 0 dB. We also note in Fig. 5(b) that rms bearing error for the PATCOR processor is relatively independent of signal direction.

We also implemented the arctan bearing estimator (derived from the arctangent of the ratio of sine-channel and cosine-channel outputs). Its performance in terms of rms error was very similar to that of the limaçon estimator when applied to our dataset.

The Cramér–Rao lower bound (CRLB) for bearings in isotropic noise;[10] is shown as a dashed line for reference in Fig. 5. This bound is an estimate of the standard deviation, which should be close to the rms error for an unbiased estimator. We do not expect this bound to be achieved in the anisotropic reverberation field, but merely note that the CR bound appears to be approached by all the estimators at SNR of 3 dB or more. For the CRLB, it should be noted that the short-time averaging creates an effective BT product of approximately 30. The formula for the CRLB, σ_θ, is taken from Eq. (14) in Ref. 10, albeit with a slight correction to the original formula:

$$\sigma_\theta \geqslant \left[2 \sum_{BT} \frac{\mathbf{s}'^T\mathbf{Q}^{-1}\mathbf{s}'\mathbf{s}^T\mathbf{Q}^{-1}\mathbf{s} - \mathbf{s}''^T\mathbf{Q}^{-1}\mathbf{s} - (\mathbf{s}'^T\mathbf{Q}^{-1}\mathbf{s})^2 - \mathbf{s}'^T\mathbf{Q}^{-1}\mathbf{s} + 4\dfrac{(\mathbf{s}'^T\mathbf{Q}^{-1}\mathbf{s})^2}{(1+\mathbf{s}^T\mathbf{Q}^{-1}\mathbf{s})}}{1+\mathbf{s}^T\mathbf{Q}^{-1}\mathbf{s}} \right]^{-1/2}, \tag{12}$$

where $\mathbf{s}' = \partial\mathbf{s}/\partial\theta$ and $\mathbf{s}'' = \partial^2\mathbf{s}/\partial^2\theta$. Specializing to the case of the three-sensor array in two-dimensional isotropic noise, we find the CRLB to be

$$\sigma_\theta \geqslant \left[\frac{12\ \mathrm{BT}\ \mathrm{SNR}^2}{1+3\ \mathrm{SNR}} \right]^{-1/2}, \tag{13}$$

where SNR is expressed as an absolute ratio, rather than in decibels, and σ_θ is in radians.

III. CONCLUSIONS

Two adaptive beamforming techniques, the PATCOR and DILBERT transform, developed for signal detection and bearing estimation in strongly directional reverberation and interference, have been described. These techniques were implemented and studied for a receiver consisting of an omnidirectional sensor and two collocated orthogonal dipole sensors. Performance was measured with recorded reverberation data. The detection performance of the PATCOR processor, as suggested by Fig. 4, was approximately 3 dB better than the benchmark limaçon beamformer at a P_{FA} of 0.01. That of the DILBERT transform, followed by a limaçon beamformer, was approximately 4 dB better, allowing for bearing variations.

The bearing-estimation performance of both the PATCOR and DILBERT processors was studied with rms error as the performance criterion. Except for signals incident on the projector–receiver axis, variable and often large reductions in rms error were observed relative to the limaçon

beamformer used as a bearing estimator. Reductions in rms bearing error up to 4× for the PATCOR processor, and up to 3× for the DILBERT processor were obtained.

As with all adaptive methods the cost of implementation must be balanced against the potential gain. The current implementation requires estimation of the data correlation matrix **Q** every 1500 samples, as well as a considerable number of matrix multiplications to generate the PATCOR processor terms or DILBERT transform coefficients. At high SNRs the extra 3 dB or so that might be obtained may not be worth the need to generate the transformation matrix and multiply each sensor measurement. In addition, with only three spatial degrees of freedom in the measurement, it is very unlikely that strong interference from more than one direction can be handled by these techniques. These points notwithstanding, the two beamformers appear to be robust when faced with real experimental data, and the improvement in detection performance alone motivates further development.

[1] R. J. Urick, *Principles of Underwater Sound for Engineers* (McGraw-Hill, New York, 1967).

[2] H. L. Van Trees, *Detection, Estimation, and Modulation Theory, Part I* (Wiley, New York, 1968).

[3] R. O. Nielsen, *Sonar Signal Processing* (Artech House, Boston, 1991).

[4] D. D. Ellis, "A shallow-water normal-mode reverberation model," J. Acoust. Soc. Am. **97**, 2804–2814 (1995).

[5] D. A. Gray, "Formulation of the maximum signal-to-noise ratio array processor in beam space," J. Acoust. Soc. Am. **72**, 1195–1201 (1982).

[6] M. Wazenski, D. Alexandrou, and D. DeFatta, "ROC evaluation of adaptive beamforming in a simulated shallow water environment," IEEE J. Ocean Eng. **21**, 94–99 (1996).

[7] I. P. Kirsteins and D. W. Tufts, "On the probability density of signal-to-noise ratio in an improved adaptive detector," ICASSP-85, 572–575, Tampa, FL (1985).

[8] L. L. Scharf and D. W. Tufts, "Rank reduction for modeling stationary signals," IEEE Trans. Acoust. Speech Signal Process. **ASSP-35**, 350–355 (1987).

[9] L. L. Scharf, "The SVD and reduced rank signal processing," Signal Process. **25**, 113–133 (1991).

[10] J. N. Maksym, "Directional accuracy of small ring arrays," J. Acoust. Soc. Am. **61**, 105–109 (1977).

#507273